"Physics of Auroral Phenomena", Proc. XLIV Annual Seminar, Apatity, pp. 92-95, 2021
© Polar Geophysical Institute, 2021

Polar Geophysical Institute

DOI: 10.51981/2588-0039.2021.44.021

CHOICE OF CONDITIONS FOR MHD SIMULATIONS ABOVE THE ACTIVE REGION, ALLOWING THE STUDY OF THE SOLAR FLARE MECHANISM

A.I. Podgorny[1], I.M. Podgorny[2], A.V. Borisenko[1], N.S. Meshalkina[3]

[1]*Lebedev Physical Institute RAS, Moscow, Russia;* e-mail: *podgorny@lebedev.ru*
[2]*Institute of Astronomy RAS, Moscow, Russia*
[3]*Institute of Solar-Terrestrial Physics SB RAS, Russia*

Abstract. Primordial release of solar flare energy high in corona (at altitudes 1/40 - 1/20 of the solar radius) is explained by release of the magnetic energy of the current sheet. The observed manifestations of the flare are explained by the electrodynamical model of a solar flare proposed by I. M. Podgorny. To study the flare mechanism is necessary to perform MHD simulations above a real active region (AR). MHD simulation in the solar corona in the real scale of time can only be carried out thanks to parallel calculations using CUDA technology. Methods have been developed for stabilizing numerical instabilities that arise near the boundary of the computational domain. Methods are applicable for low viscosities in the main part of the domain, for which the flare energy is effectively accumulated near the singularities of the magnetic field. Singular lines of the magnetic field, near which the field can have a rather complex configuration, coincide or are located near the observed positions of the flare.

Introduction

The primordial release of flare energy high in the solar corona (at heights of 1/40 - 1/20 of the solar radius [1]) is explained by the mechanism of S.I. Syrovatsky [2], according to which the flare energy is accumulated in the magnetic field of the current sheet. In the course of quasistationary evolution, the current sheet transfer into an unstable state [3]. As a result of the instability of the current sheet, a rapid release of magnetic energy occurs with the observed manifestations, which are explained by the electrodynamical model of the flare proposed by I.M. Podgorny [4]. According to the electrodynamic model, the hard X-ray emission from the flare in the lower dense layers of the solar atmosphere is explained by the acceleration of electrons in field-aligned currents caused by the Hall electric field in the current sheet. An electrodynamic model of a solar flare is proposed on the basis of the results of numerical MHD simulation and observations; analogies are used with the electrodynamic model of a substorm proposed by the author based on measurements on the Intercosmos-Bulgaria-1300 spacecraft [5]. The study of the physical mechanism of a solar flare is impossible without MHD simulation of the flare situation above a real active region, in which the magnetic field measured in the photosphere is used to set the boundary conditions, and the calculation begins several days before the flare, when the flare energy has not yet been accumulated in the magnetic field of corona. When setting the problem, no assumptions were done about the flare mechanism.

Method for the numerical solution of MHD equations

An absolutely implicit upwind finite-difference scheme which is conservative relative to magnetic flux has been developed; it was implemented in the program PERESVET. Methods for approximating MHD equations by finite-difference equations are used to ensure that the scheme remains stable at the maximum possible time step in order to speed up the calculation. The scheme is solved by the iteration method. To obtain the correct development of physical processes in time, it is necessary to carry out MHD simulation in the real scale time. Despite the use of specially developed methods, the calculations are slow. **There is a need to use parallel computing.** Parallelization of computations was carried out using CUDA technology on modern graphics cards V100 (Volta-100), P100 (Pascal-100), Titan-100. The use of the modern language Fortran PGI (Portland Group - Fortran, created specifically for parallelization using GPU graphics cards) made it possible to apply the special methods of optimizing the parallelization. The time of calculation of evolution of the field and plasma in the solar corona above the active region is determined by the size of the time step (at which the scheme remains stable), by the number of iterations and by the time of calculation of one iteration.

Choice of parameters of MHD equations. Stabilization of instabilities arising near the boundary

Due to the difficulties in matching the solution in the computational domain with the values specified at the boundary, a calculation in the real scale time can lead to the development of a strong instability that has time to develop during a long time interval, both near the photosphere and non-photospheric boundaries. The strongest

instabilities arise at low viscosities. The problem of stabilization of instabilities arising at the boundaries of the computational domain was almost completely solved [6, 7], for which artificial limitation of the rate of plasma inflow into the computational domain through the non-photospheric boundary, the setting of artificial viscosity near the non-photospheric boundary, and other stabilization methods were used. The viscosities were set in accordance with the principle of limited modeling [8], according to which much larger or much smaller units, dimensionless parameters remain much larger or smaller than units when simulated without their exact preservation.

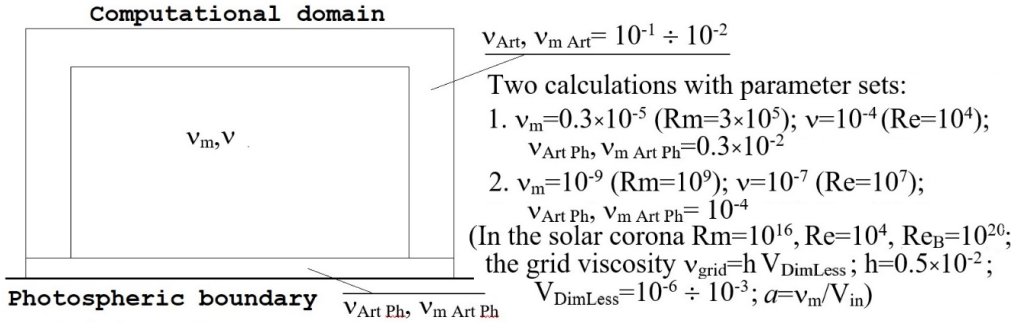

Figure 1. Viscosity and artificial viscosity for two calculation variants.

For the active region AR 10365, two calculations were carried out for two sets of parameters corresponding to relatively high and low viscosities within three days (see Fig. 1.). In both calculations near the non-photospheric boundary, to stabilize the numerical instability, sufficiently large artificial viscosities were taken, their dimensionless values (inverse to the Reynolds numbers) are ν_{Art}=ν_{mArt}=10^{-1}÷10^{-2}. In the first variant, the viscosities were taken equal to ν_m=0.3×10^{-5} (Rm=3×10^5); ν=10^{-4} (Re=10^4), the artificial viscosity near the boundary was taken relatively high$\nu_{Art\ Ph}$, $\nu_{m\ Art\ Ph}$=0.3×10^{-2}. With these parameters, due to the suppression of the perturbation propagating from the photosphere by the artificial viscosity, a sufficiently intense accumulation of the flare energy does not occur in the region; therefore, a calculation with the second set of parameters with significantly lower viscosities was required. The calculation results with these parameters are given in [6, 7]. In the second variant of the calculation, a set of parameters was selected ν_m=10^{-9} (Rm=10^9); ν=10^{-7} (Re=10^7); $\nu_{Art\ Ph}$, $\nu_{m\ Art\ Ph}$= 10^{-4}, the simulation results with these parameters are presented in the next chapter. If instabilities did not arise at the boundary, then, proceeding only from the need to obtain a stable solution inside the region, it is possible to make the following estimate of the computation time of one day of evolution in the solar corona above the active region. The time step from the Courant condition τ_K=h/(V_{MV}+V_{MA}) in the calculations is τ_K = 10^{-8}÷ 10^{-7} days. To estimate the computation time with a step τ_K : the computation time of one iteration on graphics cards using the CUDA technology is 2×10^{-2} sec, for 5 iterations the computation time of one step is 0.1 sec, so that (day ~ 10^5 sec) the computation time of one day of evolution in the solar corona is 10 - 100 days.

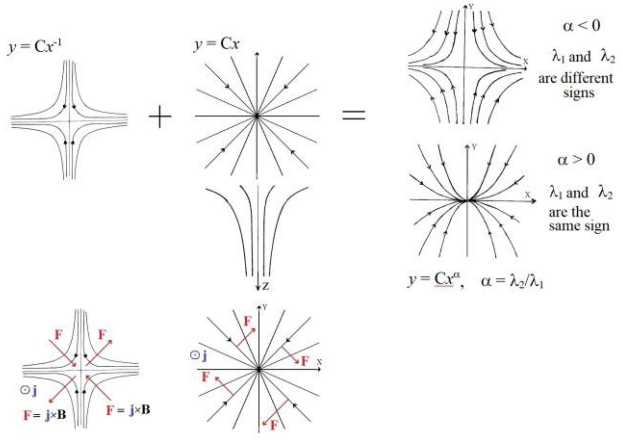

Figure 2. Superposition of X-type magnetic field and diverging magnetic field.

At low viscosities, strong disturbances arise in some places of the computational domain. These disturbances are propagating towards the boundary. The perturbations are so strong that, despite setting a large artificial viscosity near the boundary and using other special methods of stabilization, they cause numerical instability. For this set of parameters to stabilize the instabilities, it is also necessary to decrease the step (less than 10^{-8} days) and increase the number of iterations (in the calculations, their number reached 60 and more). As a result, the calculation time is greatly increased, reaching several months.

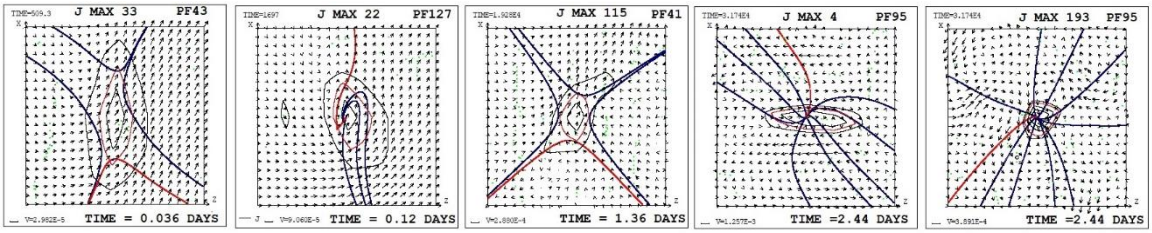

Figure 3. Examples of superposition of X-type and diverging magnetic field obtained from MHD simulation.

MHD simulation results. Complex singular line field configuration. Flare M1.4 27.05.2003 at 2:43

MHD simulation above AR 10365 showed the appearance of singular lines in which a diverging magnetic field is superimposed on the configuration of the X-type magnetic field (Fig. 2, 3, 4). Magnetic forces in X-type configuration collect disturbances into current sheet and for diverging magnetic field cause rotation of plasma around the singular line (Fig. 2). The diverging magnetic field can be large, it can dominate the X-type field, fundamentally distorting its configuration. However, even in this case, the presence of the X-type configuration leads to the accumulation of perturbations with the formation of a current sheet, in the magnetic field of which the flare energy is accumulated. In this case, even with a significant dominant diverging magnetic field, a sufficiently powerful current sheet may appear (Fig. 3, J Max 4), leading to the appearance of not only a weak flare, but also a flare of medium power.

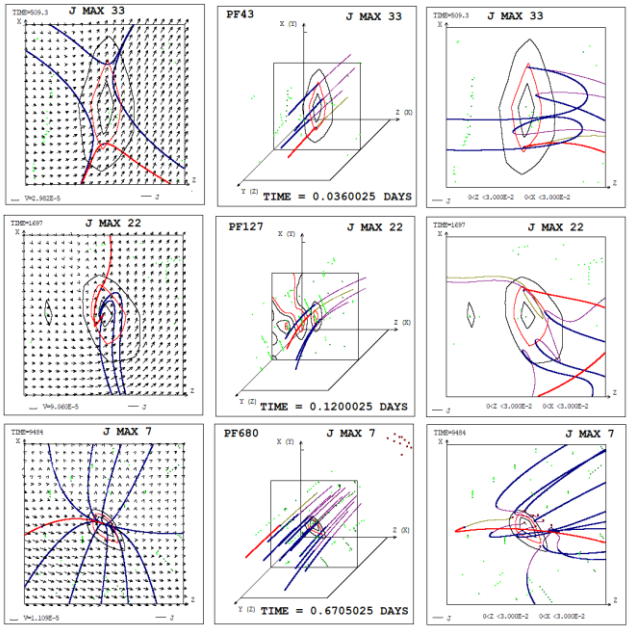

Figure 4. Field configurations near singular lines. Flat magnetic lines, three-dimensional configurations, projections of field lines on the plane of configuration.

When the X-type field and the diverging field are superimposed (Fig. 2), the magnetic lines of the resulting field have the form $y = Cx^{\alpha}$, where $\alpha = \lambda_2/\lambda_1$, λ_1 and λ_2 are the eigenvalues of the matrix $(\nabla \mathbf{B})$ [9]. If the X-type field dominates, then the magnetic lines have the form of hyperbolas ($\alpha < 0$, $\lambda_1$and $\lambda_2$have different signs). If the diverging field dominates, then the magnetic lines have the shape of parabolas ($\alpha > 0$, λ_1 and λ_2 of the same sign). Most often, the three-dimensional configuration of the magnetic field in the vicinity of the singular line is complex (examples are shown in Fig. 4), from this configuration it is impossible to determine that the line is singular. Therefore, a specially developed system for finding points through which singular line pass is required [10, 11].

In Fig. 5 shows the configuration of the magnetic field in the computational domain of corona at the time of the M 1.4 flare on May 27, 2003 at 2:43 am, which corresponds to 2.24 days from the beginning of the calculation. The current density maxima found by the graphical search system through which singular magnetic field lines can pass are indicated by green dots. The positions of the current density maxima in the region are shown, their projections onto the central plane, which passes through the central point of the computational region and is located perpendicular to the photosphere and parallel to the solar equator. Many of the current density maxima in the picture plane are the located close to the thermal X-ray source. The 193rd maximum of the current density is located in the central region of the source (all the maxima are numbered in decreasing order). The 4th maximum near the source of

thermal X-ray radiation has the most powerful current sheet. The field configurations near the 193rd and 4th current density maxima (Fig. 6) show the dominance of the diverging magnetic field over the X-type field. MHD simulation showed the coincidence of the positions of some current density maxima with the position of the source of the flare thermal X-ray radiation; the maximum of the current density with a sufficiently powerful current sheet is located at a distance of ~ 10" from the source. In the future, it will be necessary to try to more accurately select the parameters for a more precise calculation.

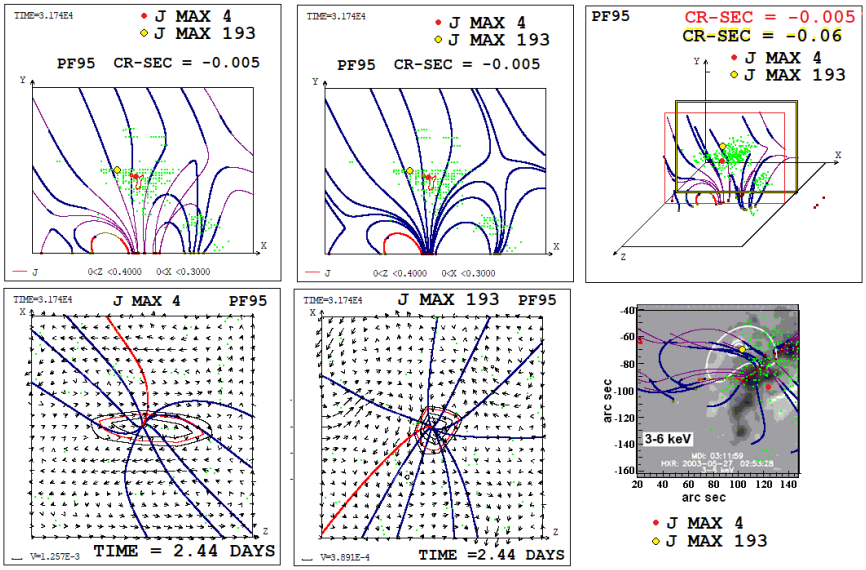

Figure 5. Three-dimensional configuration of the magnetic field in the computational domain, projection of magnetic lines on the central plane and flat magnetic lines at the time of the M 1.4 flare. The 4th and 193rd maxima of the current density are marked; other current density maxima are shown by green points. In the picture plane: magnetic field configuration, current density maxima and the distribution of soft X-ray emission of 3-6 keV, received by the RHESSI spacecraft during the M 1.4 flare on May 27, 2003 (http://rhessidatacenter.ssl.berkeley.edu) are superimposed. Magnetic field configurations and fields of velocity near the 193rd and 4th current density maxima.

Conclusion

1. To understand the physical processes causing the flare situation, simulation in the real scale of time is necessary, and the calculation should begin several days before the flare. An absolutely implicit upwind finite-difference scheme was developed, which is conservative with respect to the magnetic flux. A technique has been developed for the numerical solution of MHD equations in the solar corona in real scale of time, which is impossible without the use of parallel computations. Methods for stabilizing instabilities have been developed.
2. The simulation performed above AR 10365 showed the formation of local maxima of the current density on singular lines of the magnetic field. The field near some singular lines has complicated structure with superimposed diverging magnetic field, but even in such configuration sufficiently powerful current sheets appear. Coincidence of current sheet positions with positions of flare emission sources support the flare mechanism based on flare energy accumulation in the magnetic field of current sheet.

References

1. Lin R.P., Krucker S., Hurford G.J. et al. (2003). Astrophys. J., 595, L69–L76.
2. Syrovatskii S.I. (1966). Zh. Eksp. Teor. Fiz., 50, 1133–1147.
3. Podgorny A.I. and Podgorny I.M. (2012). Geomagn. Aeron. (Engl. Transl.), 52, 150–161.
4. Podgorny I.M., Balabin Yu.V., Vashenuk E.M., Podgorny A.I. (2010). Astronomy Reports, 54, 645–656.
5. Podgorny I.M., Dubinin E.M., Israilevich P.L., Nicolaeva N.S. (1988). GRL, 15, 1538–1540.
6. Podgorny A.I., Podgorny I.M., Borisenko A.V. (2020). Proc. 43 Annual Seminar "Phys. of Auroral Phenomena", Apatity, 56–59.
7. Podgorny A.I., Podgorny I.M., Borisenko A.V. (2020). Proc. 12-th Workshop “Solar Influences on the Magnetosphere, Ionosphere and Atmosphere”, Primorsko, Bulgaria, June, 2020, 93–98.
8. Podgorny I.M. (1978). Simulation Studies of Space. Fundamentals of Cosmic Physics, 1, №1. 1–72.
9. Podgorny A.I. (1989). Solar Physics, 123, 285–308.
10. Podgorny A.I., Podgorny I.M. (2013). Sun and Geosphere, 8(2), 71–76.
11. Podgorny A.I., Podgorny I.M. (2013). Proc. 36 Annual Sem. "Phys. of Auroral Phenomena", Apatity, 117–120.